Accepted for publication in J. Mag. Mag. Mater. (2010).

$L1_0$-ordered high coercivity (FePt)Ag-C granular thin films for perpendicular recording

Li Zhang, Y.K. Takahashi, A. Perumal, and K. Hono

National Institute for Materials Science, 1-2-1 Sengen, Tsukuba 305-0047, Japan

ABSTRACT

We report (FePt)Ag-C granular thin films for potential applications to ultrahigh density perpendicular recording media, that were processed by co-sputtering FePt, Ag and C targets on MgO underlayer deposited on thermally oxidized Si substrates. $(FePt)_{1-x}Ag_x$-$y$vol%C ($0<x<0.2$, $0<y<50$) films were fabricated on oxidized silicon substrates with a 10 nm MgO interlayer at 450°C. We found that the Ag additions improved the $L1_0$ ordering and the granular structure of the FePt-C films with the perpendicular coercivity ranging from 26 to 37 kOe for the particle size of 5 to 8 nm. The $(FePt)_{0.9}Ag_{0.1}$-50vol.%C film showed the optimal magnetic properties as well as an appropriate granular morphology for recording media, *i.e.*, average grain size of D_{av} = 6.1 nm with the standard deviation of 1.8 nm.

Keywords: FePt granular thin film, $L1_0$ ordering, magnetic perpendicular recording media

*Corresponding Author: K. Hono, kazuhiro.hono@nims.go.jp

1. Introduction

$L1_0$ ordered FePt granular thin films are considered as the most promising candidates for heat assisted perpendicular magnetic recording (HAMR) media with the recording density exceeding 1 Tbit/in^2. The high magnetocrystalline anisotropy ($K_u \sim 7\times10^7$ erg/cc) of the $L1_0$ FePt phase allows to reduce the grain size as small as 4 nm without thermal instability of magnetization [1-3], and the high coercivity resulting from the single domain $L1_0$-FePt particles can be overcome by heating during the HAMR writing process. For the practical application of FePt films as magnetic recording media, the thin film structure has to be optimized in four aspects: excellent alignment of the *c*-axis normal to the film plane, relatively small grain size with a narrow size distribution, a controllable perpendicular coercivity for writability. It is also important that the above granular structure can be processed on a soft underlayer (SUL) deposited on glass substrates. The earliest studies of FePt thin films focused on the growth of continuous polycrystalline films and their magnetic properties [4-7]. One of the problems pointed out in these investigations was the need of high temperature annealing (~600°C) for making the as-sputtered $A1$ structure ordered to the $L1_0$ structure [4]. To reduce this kinetic ordering temperature, various additives have been investigated using continuous polycrystalline films [7-14], and Cu and Ag had been found to be effective in reducing the ordering temperature.

The second stage of the FePt thin film studies was to grow granular thin films. One of the earliest investigations by Watanabe et al reported that the $L1_0$ ordering is accompanied by the coarsening of FePt nanoparticles [15]. Thereafter, many attempts have been made to fabricate $L1_0$ ordered FePt granular films without particle coarsening or sintering, e.g. choice of various spacer materials to separate FePt grains like C, SiO_2, Al_2O_3, MgF_2, TiO_2, and Ta_2O_5 [15-21] . However,

the degree of $L1_0$ order in FePt films was found to decrease when the grain size was decreased below 4 nm [15]. Although the Ag addition into FePt thin films has been known to improve the $L1_0$ ordering [11], little attention has been paid on the effect of Ag addition on the ordering and structure of *granular* FePt thin films.

We have recently reported that FePt-C granular films show excellent particle isolation and narrow size distribution with a strong perpendicular anisotropy when sputter deposited on (001)-textured MgO interlayer on thermally oxidized silicon substrate [19]. However, the substrate temperature for the growth of the $L1_0$ FePt phase was 500°C. In order to apply those granular films for hard disk drives, it is essential to grow such films on glass substrates. Hence, the purpose of this work is to investigate the influence of Ag addition on the morphology and magnetic properties of granular FePt-C thin films. We studied a series of $(FePt)_{1-x}Ag_x$-*y*vol.%C thin films deposited at a relatively low temperature of 450°C, which is lower than the softening temperature of of an alumino silicate glass, 963°C. Through this effort, we demonstrate that Ag cosputtering with FePt-C granular films improves the $L1_0$ ordering of FePt particles at a substrate temperature of 450°C with excellent granular structure having an average grain size of 5~8 nm. The films also show good perpendicular magnetization behavior.

2. Experiments

A series of *a*-SiO_2/MgO(10nm)/$(FePt)_{1-x}Ag_x$-C(vol.*y*%) ($0<x<0.2$, $0<y<50$) films were fabricated on thermally oxidized silicon (*a*-SiO_2) substrates using an ultrahigh vacuum magnetron and RF cosputtering machine. The thickness of FePt layers was fixed as 4 nm. The Ag fraction *x* and C volume fraction *y* were adjusted based on the precalibrated sputtering rates of

FePt, C, and Ag. During deposition, the base pressure of the chamber was better than 1×10^{-6} Pa. First, the MgO layer was deposited at 100°C by RF sputtering under 1.3 Pa Ar gas pressure, with a deposition rate of 0.033 nm/sec. Subsequently, FePt-Ag-C films were deposited by co-sputtering Fe, Pt, Ag, and C on the *a*-SiO_2/MgO at 450°C under 0.3 Pa Ar. The deposition rate of the FePt layer was fixed at 0.014 nm/sec. The crystalline structure and the $L1_0$ ordering of those films were examined by the standard x-ray diffraction (XRD) technique. Their magnetic properties were measured through a superconducting quantum interferometer device (SQUID), Quantum Design MPMS with the applied magnetic field up to ±55 kOe. We employ a FEI Technai F30 transmission electron microscope (TEM) to observe the microstructure of those films. The distribution of Ag and C in the films was analyzed qualitatively through electron energy-loss spectroscopy (EELS) by the post column imaging filtering technique using a Gatan Trideam imaging filter.

3. Results

Figure 1 shows XRD patterns of the *a*-SiO_2/MgO/$(FePt)_{1-x}Ag_x$-*y*vol.%C films for $0\le x\le0.2$ and $0\le y\le50$. All the peaks are indexed with $L1_0$-FePt and MgO. As to the MgO interlayer, all the films show only the MgO(002) peak at $2\theta = 43^o$, suggesting the development of strong (001) texture of MgO crystals. The (001) superlattice reflection and the (002) fundamental reflection of the $L1_0$-FePt are clearly observed in the XRD profiles, suggesting that the $L1_0$-FePt crystals are also (001) textured. This is considered to be due to the epitaxial growth of the FePt on the MgO (001) textured grains of the 10 nm interlayer [18]. In order to compare the degree of $L1_0$ ordering with various Ag fractions and C volume fractions, we plotted the intensity ratio of FePt(001) and

FePt(002) peaks as a function of Ag fraction and C volume fraction as shown in Figure 2. We found that both Ag and C cosputtering resulted in increase of the $L1_0$ ordering in the FePt film. With a fixed value of C volume fraction, *i.e.*, y=0%, 15%, and 35%, the ratio of $I_{(001)}/I_{(002)}$ increases with increasing Ag fraction x. However, for y=50%, the value of $I_{(001)}/I_{(002)}$ increases at x=0.1, then drops at x=0.2. For the fixed value of x, $I_{(001)}/I_{(002)}$ increases with increasing y, with the exception of y=50% and x=0.2. In our previous work on FePt-C without Ag, the increase of C concentration resulted in the reduction of the $L1_0$ ordering of FePt films [19]. Therefore, we believe that Ag plays more important role than C in enhancing the $L1_0$ ordering of the FePt-C granular thin films.

Figure 3 shows perpendicular and in-plane M-H loops of $(FePt)_{1-x}Ag_x$-$y$vol.%C films with various x and y. The magnetization M in plots was calculated from the measured magnetic moments divided by the volume of the film. This volume includes the contribution of Ag and carbon as well as the 4 nm FePt layer. The results show that the films have high perpendicular coercivity of 26-37 kOe, indicating high degree of $L1_0$ orders of FePt films with both Ag and C additions, which is consistent with the XRD results in Figure 2. The in-plane M-H loops show a nearly linear behavior, with coercivities < 10 kOe. It indicates that the c-axis of these films is predominantly normal to the film plane. The M-H curves also show that the increase of y leads to the decrease in the in-plane coercivity from 10 to 5 kOe. For a clear comparison of their perpendicular coercivity H_C and anisotropy K_u, we present separate plots to show the H_C and K_u as a function of x and y in Figure 4. Here K_u was calculated from the formula, $K_u = M_S^* H_k/2$, where M_S^* is the saturation magnetization of $(FePt)_{1-x}Ag_x$ particles estimated from the volume fraction of the particles, and H_k is the anisotropy field, which is derived from the saturation field of the in-plane loop [18]. Note that M_S^* is larger than the saturation magnetization M_S in the M-H

loop in Figure 3 because the carbon volume in the film is not counted for the estimation of M_S^*. We explain that carbon does not enter the FePtAg grains, which will be shown in the TEM images later. Although the carbon atom could reduce the $L1_0$ ordering of FePt particles due to the surface effect, our grain size is still much greater than the limitation value, 1.5 nm, which will be discussed in later part. Viewed from the XRD in Figure 1, the $L1_0$ ordering of FePt films increases with reducing grain size by carbon addition. Therefore, we only calculate the perpendicular anisotropy of the grain, not the whole film. This is consistent with the analysis of thermal stability of nanoparticles in magnetic recording media [3]. From Figure 4, we found that H_C increases with increasing x and y, which is consistent with the XRD results in Figure 2. The H_C reaches the maximum value of 37 kOe at x=0.1 and y=50. Note that the some of the magnetization curves do not appear to be fully saturated, so the coercivity may be even higher than 37 kOe. As for the perpendicular anisotropy K_u, we found that it decreases with carbon volume fraction y at no Ag case x=0. With Ag addition (x=0.1 and 0.2), K_u increases with y, and reaches the maximum value of 4.2×10^7 erg/cc at x=0.1 and y=50, suggesting that Ag addition enhances the degree of $L1_0$ ordering. Therefore, x=0.1 and y=50 is the optimized value for $(FePt)_{1-x}Ag_x$–$y$vol.%C film from both H_C and K_u. Because all the K_u values are in the range of $2\sim4\times10^7$ erg/cc, all those films are suitable for ultra-high density PMR media with excellent thermal stability.

Figure 5 shows bright field TEM images for the plane view of $(FePt)_{1-x}Ag_x$-$y$vol.%C films with various x and y. The histogram of grain size distribution for three films with C 50% is displayed in Figure 6. We found that without C cosputtering, the grain size is about 16-18 nm for various Ag contents. The increase of x from 0 to 0.2 results in the decrease of the grain size from

18 to 16 nm. With increasing y, the grain size decreases. At y=50%, the grain size reaches 4.8-7.9 nm. However, the grain size increases from 4.8 to 7.9 nm by increasing x= 0 to 0.2 for the films with y=50. At x=0.1 and y=50, which are regarded the optimized values, the grain size is 6.1±1.8 nm. This is close to the grain size of current CoCrPt-SiO_2 based PMR media, 6-8 nm [22-24]. By comparing the morphology of FePt grains in those images, we found that the spacing between the grains is reduced with increasing y. For $y \leq 35$, there is distinct spacing among those grains; with increasing y, the grains become more densely packed. The thickness of FePt layer is fixed as 4 nm based on the deposition rate; hence, the total thickness of $(FePt)_{1-x}Ag_x$-$y$vol.%C films increases with increasing x and y, with a maximum value of 6.8 nm at x=0.2 and y=50. Perumal et al demonstrated that 6.5 nm is a critical thickness value in FePt-C films to maintain a single magnetic layer [19]. When the thickness is below 6.5 nm, FePt grains are grown on MgO grains epitaxially; while the FePt grains begin to form double or multiple layers above 6.5 nm. The average grain size of a series of films is summarized in Figure 7 together with their standard deviation. Considering the value of K_u shown in Figure 4, we believe that $(FePt)_{0.9}Ag_{0.1}$-50vol.%C is the best choice for recording media application.

Figure 8 shows (a) enlarged plan-view TEM image, (b) cross-sectional TEM image, and (c) high resolution image of the cross section of the $(FePt)_{0.9}Ag_{0.1}$-50vol.%C film. The excellent granularity of the film having the average grain size of 6.1 nm with the standard deviation of 1.8 nm can be clearly seen. The cross sectional TEM image indicates that the $(FePt)_{0.9}Ag_{0.1}$ particles are grown on the top of MgO polycrystalline underlayer and the HREM image shows that the particles are epitaxially grown on the MgO grains with the orientation relationship of (001), having c-axis perpendicular to the plane.

Figure 9 shows the typical energy filtered TEM images of a $(FePt)_{0.8}Ag_{0.2}$-50vol.%C film. The intensities for Ag, Fe and Pt atoms are all higher in the FePt particles, suggesting the Ag is dissolved in the FePt particles as reported previously by Platt et al and You et al [11-12]. However, this is contradictly to the idea that Ag atoms are rejected from FePt, by which the kinetics for ordering is enhanced [11]. The intensity of C map is stronger in the surrounding area, suggesting C form intergranular phase that isolates $(FePt)_{0.8}Ag_{0.2}$ particles.

4. Discussion

This work has demonstrated that a perpendicular $(FePt)_{0.9}Ag_{0.1}$-50vol%C granular film with an average particles size of 6.1 nm can be processed on thermally oxidized silicon substrates with a sputtered MgO interlayer. The perpendicular anisotropy was achieved due to the expitaxial growth of the $L1_0$-$(FePt)_{0.9}Ag_{0.1}$ particles on the strongly (001)-textured MgO interlayer that was sputter deposited on a thermally oxidized silicon substrate. This film has an in-plane coercivity of 5 kOe. Based on the industry requirement on PMR media, the in-plane coercivity should be further reduced. Because of the alloying with Ag, relatively strong $L1_0$ order was achieved at the substrate temperature of 450°C, which is lower than the softening temperature of alumino silicate glass 963^{o}C. Since the $(FePt)_{0.9}Ag_{0.1}$ particles are of single domain size, the coercivity of the film was as high as 37 kOe, which is too high to switch using the currently available pole materials of write heads performing at room temperature. Therefore, a basic requirement for current recording medium is that it has a reasonably high coercivity of 5~10 kOe, with a saturation field < 20 kOe. However, since the coercivity can be tuned by reducing the degree of $L1_0$ order or by using exchange-coupled layer on the granular media, the process to fabricate high perpendicular

anisotropy FePt granular film should be applicable to processing the PMR media with appropriate soft underlayer (SUL). On the other hand, high coercivity in those granular films will not be a problem for the proposed heat-assisted magnetic recording (HAMR) [25-27]. Since the granular films were proven to be grown on sputtered MgO interlayer on thermally oxidized silicon substrate, which has an amorphous oxidization layer on the top of crystalline silicon substrate, it should be possible to grow on amorphous soft underlayer. Perumal et al proposed FeTaC amorphous SUL, which are crystallized by annealing to nanocrystalline soft magnetic FeTaC [28]. With the combination of these heat resistant SUL, the present granular film has a potential to be used as perpendicular recording media.

It has been known that Ag addition to FePt decrease the ordering temperature from $A2$ to $L1_0$ in the continuous films [11]. As to the effect in granular films, Seki et al reported that Ag addition to FePt-SiO_2 granular film has an effect of enhancing the $L1_0$ ordering, but the perpendicular anisotropy was lost on the MgO substrate [13]. In this work, we confirmed the effect of Ag in enhancing the degree of $L1_0$ ordering at 450°C, but we did not observe the degradation of the perpendicular alignment of the *c*-axis. In an early investigation, Ag was reported to diffuse out of the FePt lattice due to its low solubility with both Fe and Pt [11]. The defects left inside the FePt lattice was thought to enhance the atomic diffusion for the $L1_0$ ordering at a relatively low temperature. In this base, Ag atoms should be rejected from the FePt grains. However, our energy filtering TEM observation in Figure 9 shows that quite a large portion of Ag atoms was dissolved in the FePt grain. Similarly, the energy filter mapping work by You et al did not show distinct evidence of Ag outside FePt grains [12]. Hence the reason for the enhanced $L1_0$ ordering by Ag alloying can be attributed to the decreased melting temperature

of the FePtAg phase. Since Ag is alloyed in FePt, the Curie temperature of the FePtAg particles are expected to be lower than that for FePt (424°C) [29], which would be beneficial for HAMR. The effect of Ag on the Curie temperature on the $(FePt)_{1-x}Ag_x$-50%C film is now under investigation.

In addition to the perpendicular coercivity and anisotropy, there are other important parameters associating with the performance of PMR media like the ratio of perpendicular and in-plane coercivities H_{C_perp}/H_{C_inp}, the squareness S (defined as the ratio of remnant magnetization and the saturation magnetization, M_r/M_S), nucleation field H_n, and α value (defined as the slope of the perpendicular M-H curve, $4\pi \bullet dM/dH$ at the point of $H=H_C$). High quality PMR media requires high H_{C_perp}/H_{C_inp} ratio, S and α values. The larger the S and α, the narrower the distribution of the switching field, which means excellent performance for PMR media [22,30]. The ideal PMR media requires S=1. All those values can be derived from the M-H loops in Figure 3. Figure 10 shows the plots of the ratio of H_{C_perp} and H_{C_inp}, squareness S and α values as functions of x and y. With increasing C volume fraction y from 0 to 50, the ratio of H_{C_perp} and H_{C_inp} increases rapidly from 2.8 to 7.4, while both S and α values decrease. That means the carbon addition into FePt thin films helps eliminate the in-plane coercivity of the recording medium, which is a positive improvement of the PMR media. On the other hand, the Ag concentration x does not have distinct effect on those parameters. This is similar to the variation of grain size, as shown in Figure 7. Thus, we can draw a conclusion that the decrease of both S and α values are mainly due to the reduction of FePt grain size and size distribution. Nevertheless, huge α values result in strong coupling between grains, which will undermine the switching field distribution. Therefore, the separation of grains is also important for PMR media.

With reducing particle size, the $L1_0$ ordering of FePt films is decreased. Theoretically, the minimum size of FePt grains with good $L1_0$ ordering can be 1.5 nm [31-33]. However, in experiments it can only reach 4 nm due to the nanoparticle surface effect. Therefore, there is still some room to improve the $L1_0$ ordering in FePt films for the recording density of 1 Tbits/in^2 and above.

In this study, we have demonstrated that a granular FePtAg-C films with perpendicular anisotropy can be processed on thermally oxidized silicon (amorphous silicide) substrates using a MgO interlayer and their magnetic properties can be optimized for perpendicular recording media both for conventional and HAMR systems. This suggests that we can process similar granular films on a soft magnetic underlayer (SUL) as long as the substrates are amorphous. In a forthcoming paper, we will demonstrate that the optimized FePtAg-C film can be grown on a commercial glass substrate with a heat resistant soft magnetic underlayer [28]. We believe that this work has shown several positive experimental results as to the feasibility of applying FePtAg-C nano-granular thin films as future high density recording media.

5. Conclusion

We have fabricated (FePt)Ag-C granular thin films on an oxidized silicon substrate through a strongly (001) textured MgO interlayer at a substrate temperature of 450°C. We have achieved high perpendicular coercivity ranging from 26~37 kOe with a squareness of nearly unity. The optimum composition of the film was $(FePt)_{0.9}Ag_{0.1}$-50vol.%C, in which a single layer $(FePt)_{0.9}Ag_{0.1}$ granular layer was grown on the MgO interlayer. The $(FePt)_{0.9}Ag_{0.1}$ grains with average grain size of 6.1±1.8 nm were epitaxially grown on MgO grains. By post-annealing the

low temperature processed film (320°C) under a magnetic field, the squareness, the slope of the demagnetization curves and the nucleation field have been substantially improved. These results are all encouraging to support the feasibility of applying FePtAg-C granular films to the next generation high density recording media.

Acknowledgement

This work was supported by World Premier International Research Center Initiative (WPI Initiative) on Materials Nanoarchitronics, MEXT, Japan.

Reference

[1] J.-U. Thiele, L. Folks, M.F. Toney, D.K. Weller, J. Appl. Phys. 84 (1998) 5686.

[2] M.L. Yan, X.Z. Li, L. Gao, S.H. Liou, D.J. Sellmyer, R.J.M. van de Veerdonk, K.W. Wierman, Appl. Phys. Lett. 83 (2003) 3332.

[3] P.L. Lu, S.H. Charap, IEEE Trans. Magn. 31 (1995) 2767.

[4] M.H. Hong, K. Hono, M. Watanabe, J. Appl. Phys. 84 (1998) 4403.

[5] T. Suzuki, K. Harada, N. Honda, K. Ouchi, J. Magn. Magn. Mater. 193 (1999) 85.

[6] S. Okamoto, N. Kikuchi, O. Kitakami, T. Miyazaki, Y. Shimada, K. Fukamichi, Phys. Rev. B 66 (2002) 024413.

[7] T. Maeda, T. Kai, A. Kikitsu, T. Nagase, J. Akiyama, Appl. Phys. Lett. 80 (2002) 2147.

[8] Y.M. Lee, B.S. Lee, C.G. Lee, B.H. Koo, Y. Shimada, J. Magn. Magn. Mater. 310 (2007) E918.

[9] Y.K. Takahashi, M. Ohnuma, K. Hono, J. Magn. Magn. Mater. 246 (2002) 259.

[10] T. Yang, K. Kang, G.H. Yu, T. Suzuki, J. Phys. D: Appl. Phys. 35 (2002) 2897.

[11] C.L. Platt, K.W. Wierman, E.B. Svedberg, R. van der Veerdonk, J.K. Howard, A.G. Roy, D.E. Laughlin, J. Appl. Phys. 92 (2002) 6104.

[12] C.Y. You, Y.K. Takahashi, K. Hono, J. Appl. Phys. 100 (2006) 056105.

[13] T.O. Seki, Y.K. Takahashi, K. Hono, J. Appl. Phys. 103 (2008) 023910.

[14] L. Castaldi, K. Giannakopoulos, A. Travlos, N. Boukos, D. Niarchos, S. Boukari, E. Beaurepaire, J. Appl. Phys. 105 (2009) 093914.

[15] M. Watanabe, T. Masumoto, D.H. Ping, K. Hono, Appl. Phys. Lett. 76 (2000) 3971.

[16] Y.K. Takahashi, T. Ohkubo, M. Ohnuma, K. Hono, J. Appl. Phys. 93 (2003) 7166.

[17] E. Yang, D.E. Laughlin, J. Appl. Phys. 104 (2008) 023904.

[18] A. Perumal, Y.K. Takahashi, T.O. Seki, K. Hono, Appl. Phys. Lett. 92 (2008) 132508.

[19] A. Perumal, Y.K. Takahashi, K. Hono, Appl. Phys. Exp. 1 (2008) 101301.

[20] J.S. Chen, B.C. Lim, Y.F. Ding, J.F. Hu, G.M. Chow, G. Ju, J. Appl. Phys. 105 (2009) 07B702.

[21] T. Klemmer, Y.G. Peng, X.W. Wu, G.P. Ju, IEEE Trans. Magn. 45 (2009) 845.

[22] Y. Tanaka, Proceedings of the IEEE 96 (2008) 1754.

[23] H.S. Lee, V.W. Guo, J.-G. Zhu, D.E. Laughlin, J. Appl. Phys. 103 (2008) 07F541.

[24] K. Srinivasan, S.N. Piramanayagam, R.W. Chantrell, Y.S. Kay, J. Magn. Magn. Mater. 320 (2008) 3036.

[25] J.J.M. Ruigrok, R. Coehoorn, S.R. Cumpson, H.W. Kesteren, J. Appl. Phys. 87 (2000) 5398.

[26] M. Alex, A. Tselikov, T. McDaniel, N. Deeman, T. Valet, D. Chen, IEEE Trans. Magn. 37 (2001) 1244.

[27] M. Mochida, M. Birukawa, T. Suzuki, IEEE Trans. Magn. 37 (2001) 1396.

[28] A. Perumal, Y.K. Takahashi, K. Hono, J. Appl. Phys. 105 (2009) 07A304.

[29] K. Barmak, J. Kim, D.C. Berry, W.N. Hanani, K. Wierman, E.B. Svedberg, J.K. Howard, J. Appl. Phys. 97 (2005) 024902.

[30] A. Berger, Y. Xu, B. Lengsfield, Y. Ikeda, E.E. fullerton, IEEE Trans. Magn. 41 (2005) 3178.

[31] B. Yang, M. Asta, O.N. Mryasov, T.J. Klemmer, R.W. Chantrell, Scr. Mater. 53 (2005) 417.

[32] R.V. Chepulskii, W.H. Butler, Phys. Rev. B 72 (2005) 134205.

[33] C.B. Rong, D. Li, V. Nandwana, N. Poudyal, Y. Ding, Z.L. Wang, H. Zeng, J.P. Liu, Adv. Mater. 18 (2006) 2984.

Figure Captions

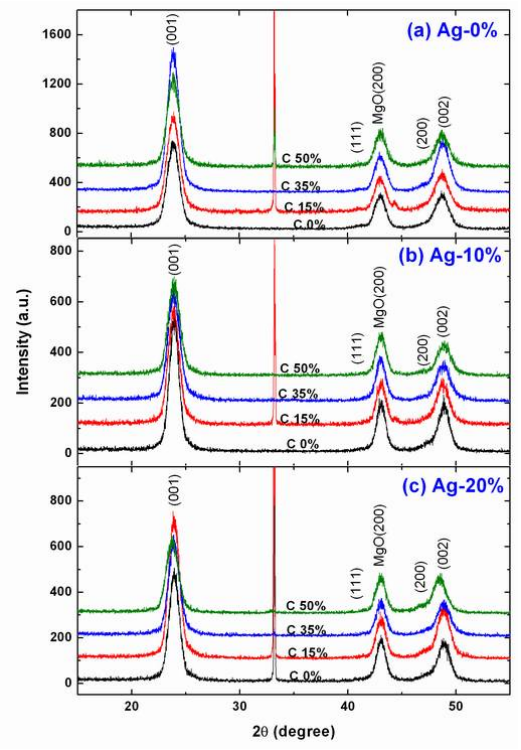

Fig. 1 XRD profiles of the $(FePt)_{1-x}Ag_x$–$y$vol.%C thin films with $0 \le x \le 0.2$, $0 \le y \le 50$

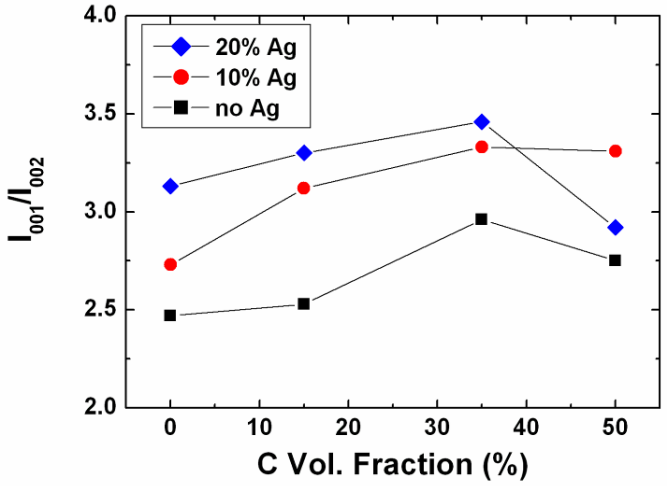

Fig. 2 XRD integral intensity ratio, I_{001}/I_{002} for the $(FePt)_{1-x}Ag_x$–$y$vol.%C thin films with $0 \le x \le 0.2$, $0 \le y \le 50$

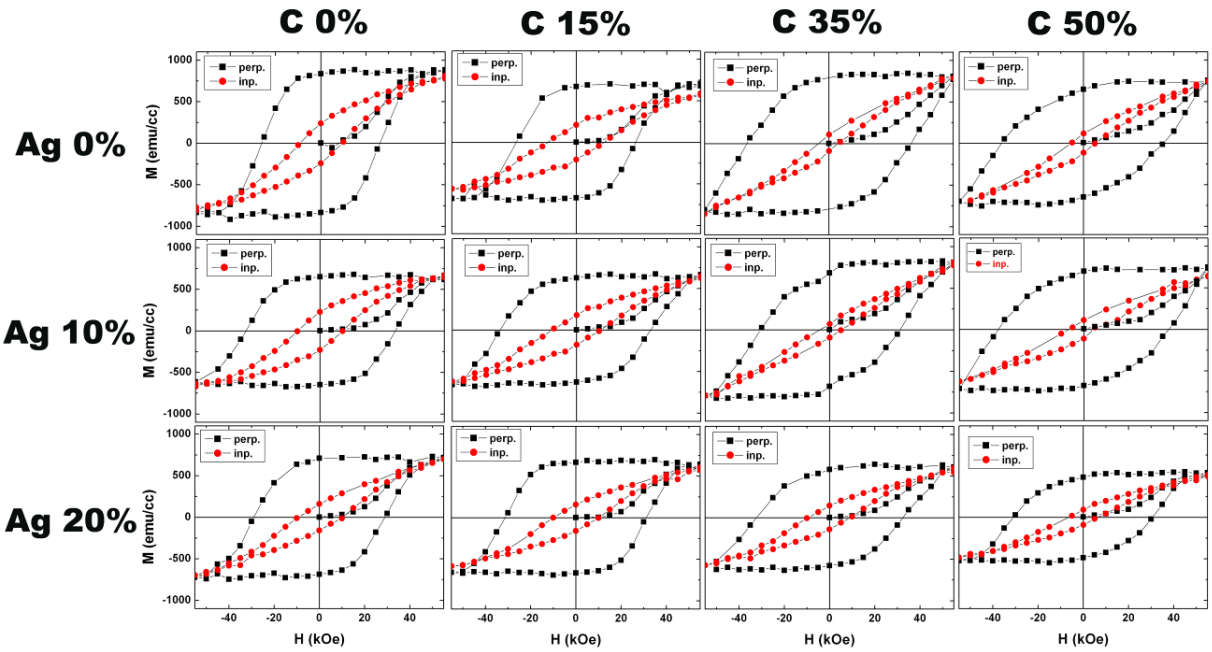

Fig. 3 Perpendicular and in-plane magnetization curves of the $(FePt)_{1-x}Ag_x$–$y$vol.%C with $0 \le x \le 0.2$, $0 \le y \le 50$

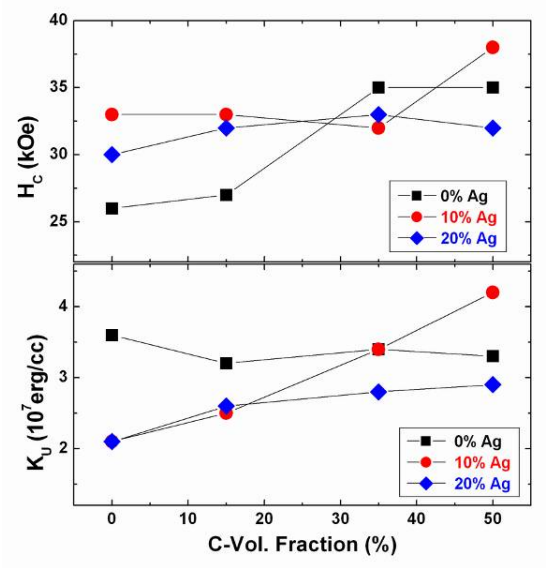

Fig. 4 Perpendicular coercivity H_C and anisotropy K_u vs. Ag and C concentration of the $(FePt)_{1-x}Ag_x$–$y$vol.%C films

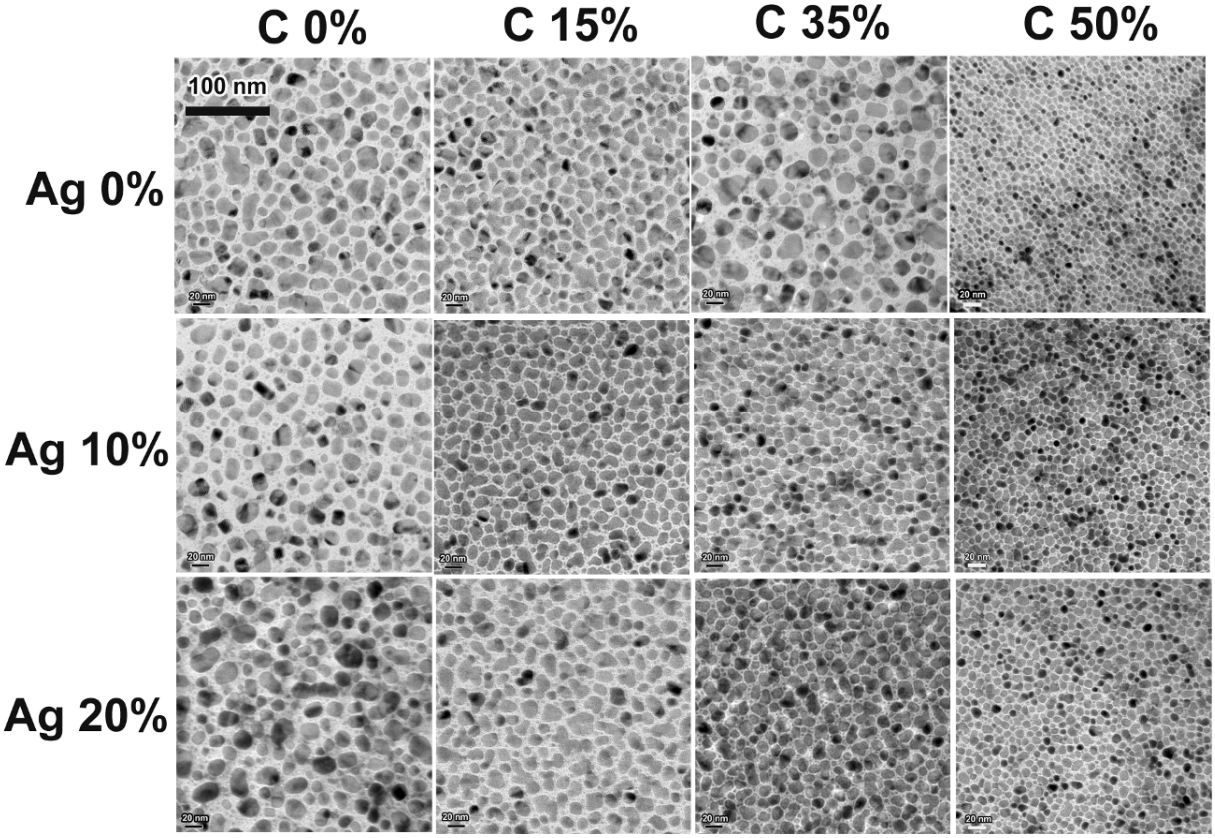

Fig. 5 Plane view bright field TEM images of the $(FePt)_{1-x}Ag_x$–$y$vol.%C films

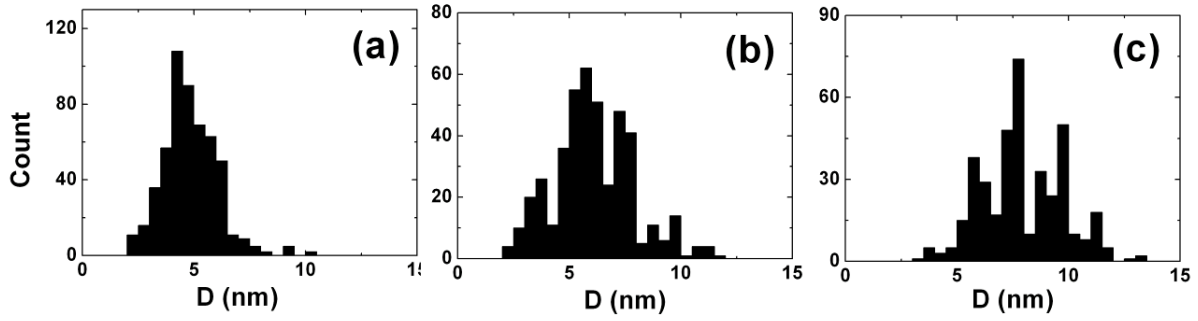

Fig. 6 Histogram of grain size distribution for three FePt-C50% films: (a) Ag 0%, (b) Ag 10%, and (c) Ag 20%

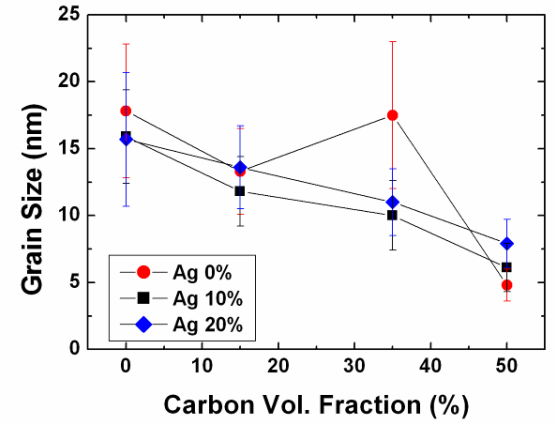

Fig. 7 Average grain size distribution of the $(FePt)_{1-x}Ag_x$−*y*vol.%C films

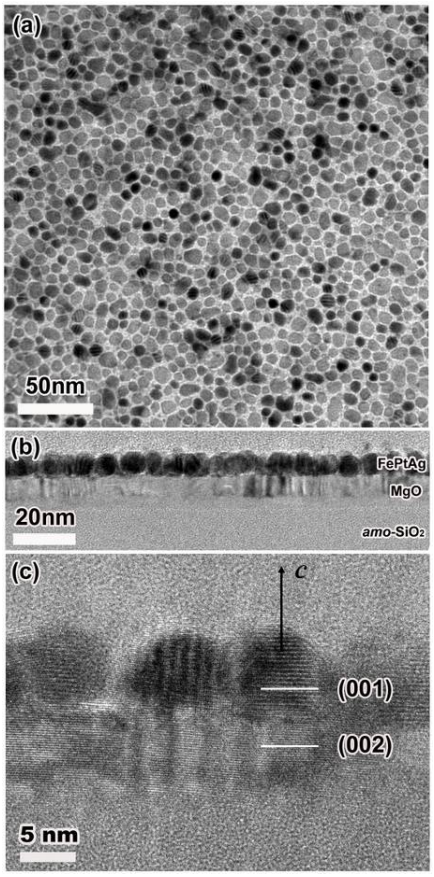

Fig. 8 (a) Bright field plane view image, (b) cross sectional bright field image, and (c) cross sectional high resolution TEM image of the $(FePt)_{0.9}Ag_{0.1}$−50vol.%C film

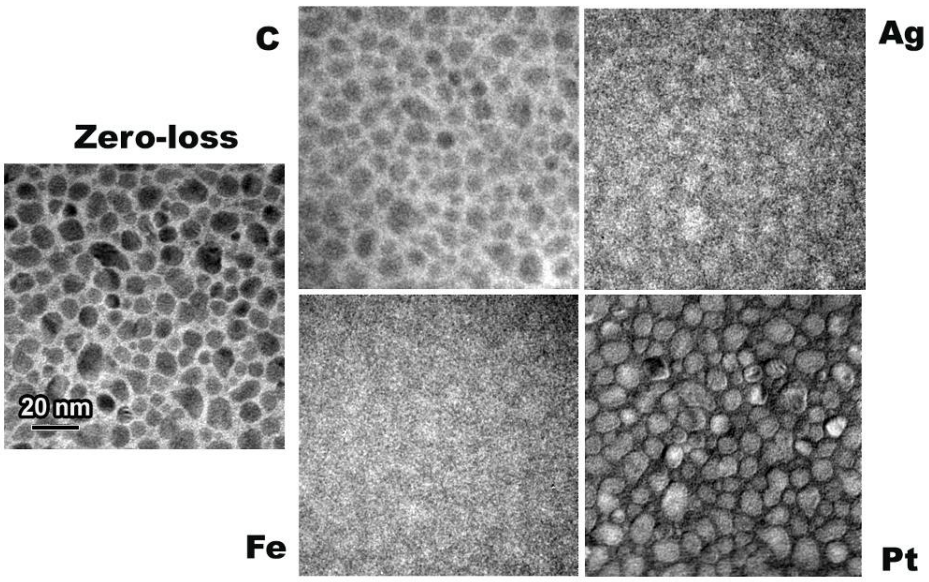

Fig. 9 Energy filtered TEM images of the $(FePt)_{0.8}Ag_{0.2}$−50vol.%C film

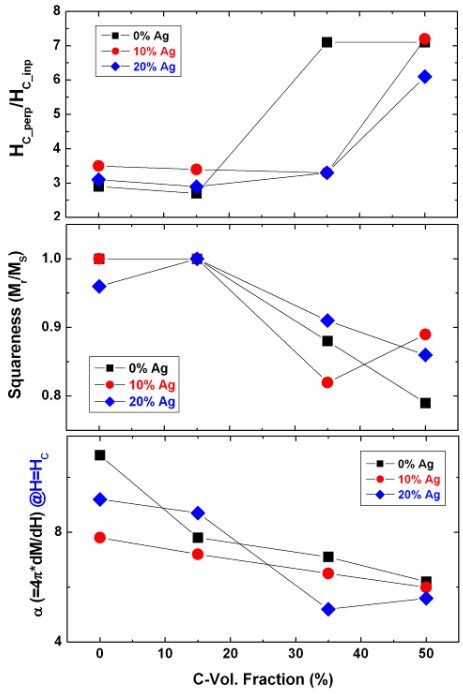

Fig. 10 Ratio of H_{C_perp} and H_{C_inp}, Squareness S, and α ($\equiv 4\pi \bullet dM/dH$ @ $H=H_C$) values of all the $(FePt)_{1-x}Ag_x$−$y$vol.%C films